Available online at www.sciencedirect.com

SCIENCE DIRECT®

Developmental Biology 273 (2004) 48–62

DEVELOPMENTAL BIOLOGY

www.elsevier.com/locate/ydbio

Yantar, a conserved arginine-rich protein is involved in *Drosophila* hemocyte development

Sergey A. Sinenko,[a,*] Eun Kyung Kim,[a,b,c] Rhoda Wynn,[d] Pascal Manfruelli,[a] Istvan Ando,[e] Kristi A. Wharton,[d] Norbert Perrimon,[b] and Bernard Mathey-Prevot[a]

[a] *Division of Pediatric Oncology, Dana-Farber Cancer Institute and Children's Hospital, Boston, MA 02115, USA*
[b] *Department of Genetics, Harvard Medical School, Howard Hughes Medical Institute, Boston, MA 02115, USA*
[c] *National Creative Research Initiative Center for Cell Death, Korea University, Seoul, South Korea*
[d] *Department of Molecular Biology, Cell Biology and Biochemistry, Brown University, Providence, RI 02912, USA*
[e] *Institute of Genetics, Biological Research Center for the Hungarian Academy of Sciences, Szeged, Hungary*

Received for publication 26 January 2004, revised 6 May 2004, accepted 7 May 2004
Available online 3 July 2004

Abstract

To identify novel factors involved in *Drosophila* hematopoiesis, we screened a collection of lethal recessive mutations that also affected normal hemocyte composition in larvae. We present the characterization of the gene *yantar* (*ytr*) for which we isolated null and hypomorphic mutations that were associated with severe defects in hemocyte differentiation and proliferation; *ytr* is predominantly expressed in the hematopoietic tissue during larval development and encodes an evolutionary conserved protein which is predominantly localized in the nucleus. The hematopoietic phenotype in *ytr* mutants is consistent with a defect or block in differentiation of precursor hemocytes: mutant larvae have enlarged lymph glands (LGs) and have an excess of circulating hemocytes. In addition, many cells exhibit both lamellocyte and crystal cell markers. Ytr function has been preserved in evolution as hematopoietic specific expression of the *Drosophila* or mouse Ytr proteins rescue the differentiation defects in mutant hemocytes.

Keywords: Hemocyte development; Melanotic masses; Lamellocytes; Lymph glands; *Yantar*; *Lozenge*

Introduction

Studies in the last two decades have revealed a strong evolutionary conservation in genes and molecular pathways involved in vertebrate and invertebrate development (Evans et al., 2003; Potter et al., 2000; Reiter et al., 2001). Despite differences in the composition of cell types, this conservation has held true for mammalian and *Drosophila* genes involved in hematopoiesis (Evans et al., 2003). The *Drosophila* hematopoietic system is primitive and largely confined to cells analogous to those of the vertebrate myeloid lineage. At the larval stage, *Drosophila* hemocytes belong to three major classes: monocytelike plasmatocytes, involved in host defense and phagocytosis; crystal cells which carry out melanization reactions; and lamellocytes that are involved in encapsulation of objects that are too big to be phagocytosed (Rizki and Rizki, 1983). The conserved transcription factors—Serpent (Srp) a GATA protein, Glial cell missing (Gcm), Ushaped (Ush), the Friend of GATA (FOG)-ortholog and Lozenge (Lz), a Runx protein with homology to mammalian AML1—have been implicated in lineage specification of hemocytes. Srp, Gcm, and Ush transcription factors are required for the maintenance and specification of early hemocyte precursor cells to the plasmatocyte lineage, while Lz plays a similar role for the crystal cell lineage (Alfonso and Jones, 2002; Fossett et al., 2001; Lebestky et al., 2000). The fact that the corresponding mammalian transcription factors (GATA-1 and -2, FOG and AML1) also play pivotal roles in vertebrate hematopoiesis validates the notion that the basic mechanisms involved in cell fate specification, survival, proliferation, and differentiation of hemocytes are conserved between flies and vertebrates. Furthermore, signal transduction pathways implicated in mammalian hematopoiesis (e.g.,

* Corresponding author. Division of Pediatric Oncology, Dana-Farber Cancer Institute, 44 Binney Street, M647, Boston MA, 02115. Fax: +1-617-632-6845.
E-mail address: sergey_sinenko@dfci.harvard.edu (S.A. Sinenko).

0012-1606/$ - see front matter © 2004 Elsevier Inc. All rights reserved.
doi:10.1016/j.ydbio.2004.05.022

JAK/STAT, NF-κB, Ras/Raf, VEGF, the Notch pathways) also participate in *Drosophila* hemocyte cell survival, proliferation, and differentiation (Cho et al., 2002; Duvic et al., 2002; Lebestky et al., 2003; Luo et al., 2002; Mathey-Prevot and Perrimon, 1998; Qiu et al., 1998). A recent study has clarified the origin of the various mature hemocytes during development (Holz et al., 2003). Similar to vertebrates, *Drosophila* has two developmentally distinct waves of hematopoiesis, embryonic and larval. In contrast to vertebrates, embryonically derived hemocytes persist throughout the larval and adult phases. Hemocytes of larval origin are released from the lymph gland (LG) toward the end of third instar and show the same diversity of cell types as hemocytes of embryonic origin (Holz et al., 2003; Lanot et al., 2001). However, the nature of the genes required for the maintenance of early hemocyte precursors and differentiation to the lamellocyte lineage remain unknown.

To address this question, we embarked on a genetic screen to identify mutants with specific defects in hemocyte differentiation. We screened over 2000 chromosomes bearing EMS-induced lethal recessive mutations for the presence of melanotic masses in mutant larvae, a phenotype often associated with defects in proliferation or differentiation of hemocytes in *Drosophila*. We recovered three independent mutations (*3A8*, *5K29*, and *5E24*) that disrupted the normal composition of circulating hemocytes in larvae. Analysis of the hematopoietic defects in these mutants suggested that the most serious and interesting phenotype was linked with the *5E24* mutation. Genetic and molecular analyses indicated that the mutation disrupted the annotated gene *CG18426* (which we call hereafter *yantar*, *ytr*); *ytr* encodes a protein with an arginine-rich domain found in a variety of RNA-binding or splicing proteins and a unique C-terminus of unknown function which shows a high degree of conservation among the identified Ytr orthologs in other species. *ytr* mRNA is dynamically expressed during embryogenesis and is highly enriched in the lymph glands and circulating hemocytes during larval development. In addition to disrupting normal hematopoiesis, loss of function mutations in *ytr* results in the stunted growth of imaginal discs and brain. Mirroring its sequence conservation, the function of Ytr has been preserved throughout evolution as ectopic expression of the mouse Ytr (m-Ytr) protein in the hematopoietic tissue of *ytr* mutants results in the full restoration of the normal hemocyte differentiation.

Materials and methods

Strains and genetics

The *5E24*, *3A8*, and *5K29* mutant alleles were generated in a large-scale mutagenesis using ethyl methanesulfonate (N. Perrimon, unpublished). An additional EMS-induced *ytr* allele, *Ae-3*, was originally isolated on the basis of its lethality when placed *in trans* with the deficiency *Df(2R)bwS46* (Wharton et al., 1999). The $bgcn^{QS2}$ allele was kindly provided by B. Ohlstein (University of Texas). All other stocks, including enhancer trap lines: $P\{w^{+mC} = UAS-mCD8::GFP.L\}LL4, y^1 w^*$ $P\{w^{+mW.hs} = GawB\}lz-Gal4$ and $w^{[*]}$; $P\{w^{[+mW.hs]} = GawB\}^{5015}$, were obtained from the Bloomington Stock Center. *Oregon-R*, w^{1118} or *ytr* heterozygous flies were used as control strains. Flies were maintained on standard *Drosophila* cornmeal/sucrose/yeast medium at 20°C, 25°C, or 29°C, as necessary.

Genetic mapping of the 5E24 mutation

Meiotic recombination analysis mapped the *5E24* mutation between the *px* and *sp* recessive markers. A *(al, dp^{ovi}, b, pr, c, px, 5E24/Cyo, GFP)* stock was established and subsequently used in deficiency mapping. Seven deletions (*Df(2R)b23*, *Df(2R)106*, *Df(2R)bwDRa*, *Df(2R)egl2*, *Df(2R)chi*, *Df(2R)or-BR*, *Df(2R)bwS4*) that uncovered the 59–61 genetic interval on chromosome II failed to complement *5E24*. Their distal breakpoints as well as that of two deficiencies (*Df(2R)OV1* and *Df(2R)x32*) that complemented our mutation were estimated using complementation with mapped lethal P insertions ($P\{w[+mC] = lacW\}l(2)^{k13214}$, $P\{w^{+mC} = lacW\}l(2)k13214^{k13214}$, $P\{ry^{+t7.2} = PZ\}ken^{02970}$, and $P\{hsneo\}l(3)neo1^1$). Taking into account the molecular mapping of *Df(2R)egl2* provided in (Wharton et al., 1999), we placed the mutation between the distal breakpoints of *Df(2R)OV1* and *Df(2R)egl2*.

Molecular analysis and excision of $P\{w + mC = lacW\}^{k13108b}$, a ytr allele

The insertion site of $P\{w + mC = lacW\}^{k13108b}$ transposon, a *ytr* allele, was determined after plasmid rescue by inverse PCR (http://www.fruitfly.org/about/methods/inverse.pcr.html). The forward primer, *P[GalW]* GCGTCGGTTTAGAGCAGCAGAGCTT, and reverse primer, *Plac1* CACCCAAGGCTC-TGCTCCCACAAT, were used to amplify an approximately 850-bp fragment. Additional *ytr* alleles (*Δ*P22*, *Δ*P2*) were isolated by imprecise excision of $P\{w + mC = lacW\}^{k13108b}$ using a stock carrying the *Δ2–3* transposase. Deletions in these *ytr* alleles were confirmed with PCR mapping and complementation with *gbb* and *eIF6* mutations.

Molecular biology

DNA from homozygous mutant or wild-type larvae was isolated and the overlapping fragments of *ytr* genomic locus were amplified using eight sets of primers. Potential changes due to allelic variation were controlled for by sequencing the *ytr* locus in $pkdt^{5K29}$ mutant which shares the same genetic background as ytr^{5E24}. Sequencing reactions were performed at the core facility at the Dana-Farber Cancer Institute. Protein domain predictions were made with BLAST (http://www.ncbi.nlm.nih.gov/BLAST/). *Kpn*I

and *Bgl*II linkers were added to the coding region of *ytr* cDNA (EST LD12325) as well as to the mouse *ytr* (*mytr*) cDNA (BF682621, IncyteGenomics) at the 5′and 3′ ends, respectively, to facilitate cloning into the pUASp vector. Transgenic lines were generated as previously described (Callus and Mathey-Prevot, 2002). To facilitate expression of HA-mYtr in mammalian cells, 5′ *Eco*RI and 3′ *Xho*I restriction sites were added to the mYtr coding region and cloned into the pcDNA3.1-KozakHAHA vector, kindly provided by Dr. H. Widlund (Huber et al., 2003).

Northern blot analysis

Drosophila polyA$^+$ RNA was prepared after Trizol reagent (Gibco-BRL) extraction and purification with PolyATract^R mRNA Isolation System IV (Promega). Northern blot hybridization was performed as described (Callus and Mathey-Prevot, 2002).

Immunocytochemistry and hemocyte counts

ytr Mutant homozygous larvae were transferred to new vials containing fresh food for 4–7 days before collecting hemocytes. To determine total hemocyte numbers in different mutants, the hemocytes from five larvae of each genotype were collected in 50 μl of Ringer solution. The resuspended cells were counted using a hemocytometer, and counts were used to determine the number of cells per single larva. To count L1-positive (L1$^+$) and Lz-positive (Lz$^+$) cells, hemocytes from 40 larvae of each genotype were collected into 400 μl of Ringer solution. A 40-μl aliquot of the hemocyte suspension (corresponding to 4 larvae) was placed on a single well of a 10-well glass slide (PGC Scientifics). Cells were let to adhere for 40 min before fixation with acetone (8 min) or 2% formaldehyde solution (20 min). Fixed cells were treated with specific antibodies, as indicated in the appropriate figure legends: anti-L1 and -H2 antibodies directed against specific hemocyte markers (previously described in Asha et al., 2003; Kurucz et al., 2003; anti-Lz antibody (kindly provided by Dr. U. Banerjee); antiphosphohistone H3-specific antibodies (Upstate). Request for L1 and H2 hemocyte-specific antibodies should be addressed to Dr. I. Ando. Biotinylated antimouse antibodies with the "ABC" system (DAKO) or FITC-labeled secondary antibodies (DAKO) were used according to the manufacturer's instructions. An equivalent area of the slide was scanned to count positive and negative cells. Multiple independent areas from the same slide were analyzed, and the analysis was repeated multiple times to ensure reproducibility. Numbers of Lz- or L1-positive cells relative to the total number of hemocytes were calculated in each case. These numbers were used to calculate back the numbers of positive cells circulating in larvae and are shown with their standard deviations. For rescue experiments, hemocytes from a single larva of each genotype were collected in 50 μl of Ringer solution in a single well of a10-well glass slide. Homozygous *ytr* mutant larvae were selected based on the absence of the balancer *CyO* chromosome (marked with GFP) and the presence of small, mutant imaginal discs. Cells were let to adhere before fixation with a 2% formaldehyde solution (Sigma). DNA was counterstained with 4′,6′-diamidino-2-phenylindole (DAPI), and final preparations were mounted in 80% glycerol in PBS. Multiple (10) independent samples for each genotype were analyzed to ensure reproducibility. Cell images were taken under different magnifications with a light (Nomarski optics) and fluorescent microscope (Zeiss Optical).

RNA in situ hybridization

A *ytr* digoxigenin (DIG)-labeled riboprobe was prepared according the kit manufacturer's instruction (Roche). In situ hybridization of staged embryos was carried out according to Protocol 12.5 of Sullivan et al. (2000). For in situ hybridization of larval tissues, third instar larvae were dissected directly in 4% formaldehyde, and subsequent steps were carried out as above. Larval hemocytes were extracted after dissection of larvae on glass slides in a drop of 4% paraformaldehyde in PBS for 20 min. Hemocytes were washed and prehybridized before the probe was added. Hybridization was performed at 55°C in a hermetically closed humid chamber (4 h to overnight). Detection was performed with anti-DIG antibody conjugated to alkaline phosphatase (Roche) (Sullivan et al., 2000).

Cell culture and transfection

NIH 3T3 and COS7 cells were cultured in RPMI supplemented with 10% FCS. Transfections were carried out with the FUGENE-6 transfection reagent (Roche) according to the manufacturer's instructions. Briefly, subconfluent cultures of cells grown on glass slides (Lab-Tek II Chamber slide system, Nalge Nunc, Int.) were transfected with 2.5 μl of the FUGENE-6 reagent containing either 0.5–1 μg of HA-mYtr-, HA-MITF-, or HA-Tsp68C-pcDNA3.1 plasmids in 200 μl serum-free RPMI. RPMI containing 10% FCS medium was added 1 h later. Twenty-four hours after transfection, cells were fixed with 3% formaldehyde in PBS for 20 min and incubated in 0.1% Tween 20, 0.3% BSA in PBS. Fluorescein-labeled HA-specific monoclonal antibodies (3F10, Roche) was added to the fixed and permeabilized cells for 2 h, and DNA was counterstained with DAPI. Cells were then examined by fluorescence microscopy (Zeiss Optical).

Results

Screen for Drosophila hematopoietic mutants

Our screen was based on the fact that distinct black masses (also known as melanotic tumors) often arise in the

larval body cavity of mutants with aberrant hematopoiesis (Alfonso and Jones, 2002; Badenhorst et al., 2002; Dearolf, 1998; Gateff, 1978). About 2000 mutant stocks were screened in this fashion, and we identified 18 EMS-induced lethal mutations defining 18 complementation groups. Three of these mutations (*5E24*, *5K29*, and *3A8*) were selected because of their reproducible and fairly penetrant melanotic tumor phenotype, and we named their corresponding genes *yantar* (*ytr*), *polka dots* (*pkdt*), and *splotchy* (*splo*). Hemocytes from these mutants were visualized after immunostaining using two hemocyte-specific monoclonal antibodies, MAb H2 and L1. MAb H2 recognizes the *hemese* antigen present in all *Drosophila* hemocytes, whereas MAb L1 is specific for lamellocytes (Asha et al., 2003; Kurucz et al., 2003). We observed a marked elevation in circulating hemocytes in ytr^{5E24} and $splo^{3A8}$ homozygous larvae (4- and 1.8-fold increase, respectively) compared to counts in wild-type or heterozygous larvae (Fig. 1 and data not shown). In contrast, the $pkdt^{5K29}$ mutant showed a 3.2-fold reduction in circulating hemocytes. In agreement with previous studies (Lanot et al., 2001; Russo et al., 2001), only 0.3% of peripheral hemocytes circulating in wild-type hemolymph were L1-positive ($L1^+$) cells (lamellocytes) (Fig. 1). In contrast, the percentage of $L1^+$ cells was dramatically increased in all three mutants they represented, 25% and 27% of circulating hemocytes in ytr^{5E24} and $pkdt^{5K29}$ mutants, respectively, and 8% in the $splo^{3A8}$ mutant. Interestingly, $L1^+$ cells from these mutants often had morphology distinct from typical lamellocytes (smaller and more round) but were usually larger than wild-type plasmatocytes. Crystal cells in wild-type and mutant larvae were readily identified based on their round morphology and the presence of paracrystalline inclusions in the cytoplasm. We did not observe dramatic differences in the relative number or morphology of crystal cells between any of the mutants and wild-type samples, suggesting that crystal cell differentiation in the mutants was largely unaffected (data not shown). As the ytr^{5E24} mutation was associated with the most pleiotropic phenotype showing a significant overaccumulation of hemocytes and an uncharacteristically high proportion of morphologically diverse $L1^+$ cells, we chose to characterize the molecular lesion in this mutant.

The gene CG18426 is affected in ytr^{5E24} mutant

Initial deficiency mapping placed the site of the ytr^{5E24} mutation between the subdivisions 59 and 60 of the right arm of chromosome II. To further narrow down the interval, we selected four deficiencies (*Df(2R)b23*, *Df(2R)egl2*, *Df(2R)x32*, and *Df(2R)OV1*) which had been characterized and used to identify other mutations in this region (Munn and Steward, 2000; Ohlstein et al., 2000; Wharton et al., 1999). Complementation studies between the ytr^{5E24} mutation and these deficiencies indicated that the mutation lied in the interval between the distal breakpoints of *Df(2R)OV1* and *Df(2R)egl2*. This interval was confirmed using *Df(2R)Chi* which overlaps with the distal region of *Df(2R)egl2* and extends further toward the telomere (Fig. 2A). Several genes mapped within or close to that interval (Fig. 2B) (Adams et al., 2000; Lukacsovich et al., 1999). We quickly ruled out *gbb* and *bgcn* by complementation. To help us identify which of the remaining genes was mutated in ytr^{5E24}, we searched for lethal P-element transposon insertions and additional EMS-induced zygotic lethal mutations in the region. We identified two P-element insertions, $P\{w + mC = lacW\}^{k13108b}$ ($P(lacW)^{k13108b}$) and $P\{w[+mC] = lacW\}l(2)^{k13214}$ ($eIF6^{k13214}$). Complementation studies indicated that the former was allelic to ytr^{5E24}, whereas the latter which disrupts the coding sequence of the *eIF6* gene (Spradling et al., 1999) complemented the ytr^{5E24} mutation. Plasmid rescue on DNA isolated from $P(lacW)^{k13108b}$ homozygous larvae revealed that the P-element was inserted in the second intron of the annotated gene *CG18426* (Fig. 2B.). To verify that the lethality associated with $P(lacW)^{k13108b}$ was linked to the transposon, we mobilized the P-element associated with $P(lacW)^{k13108b}$ and isolated flies which had lost the P-element. Stocks derived from precise excisions were homozygous viable and fertile, and showed no hematopoietic defects. Along with the precise excisions of the P-element $ytr^{k13108b}$, we isolated several imprecise excision lines. As expected, two of them (*ΔP2*, *ΔP22*) failed to complement ytr^{5E24} and $ytr^{k13108b}$, but complemented $eIF6^{k13214}$, *gbb*, and *bgcn* mutations. In addition, four EMS-induced mutations belonging to the F complementation group reported in Wharton et al. (1999) were tested by complementation. Three of them, including ytr^{Ae-3}, failed to complement ytr^{5E24} and $ytr^{k13108b}$ but complemented mutants in *eIF6* and *gbb*. These data indicate that *CG18426* is the affected gene in ytr^{5E24} mutants. The appearance of mutant pupae with melanotic masses reminded us of amber with inclusions, and we named the gene *yantar* (amber in Russian).

Characterization of molecular lesions associated with the ytr alleles

ytr Resides in a locus densely packed with genes (Lukacsovich et al., 1999). It lies next to *gbb* in a head-to-head orientation, 453 bp from the initiating ATG codon of *gbb*. The single exon gene *eIF6* is located in the third intron of *ytr*, in the same orientation as *ytr* (Fig. 2B). Sequences from a *ytr* cloned expressed sequence tag (EST) (*LD12035*, *AY061143*) and a *ytr* cDNA isolated from a *Drosophila* embryonic cDNA library (*cDNA11*, *AY171243*) revealed that the two clones differed in their use of 5′ untranslated exons but encoded the same open reading frame (ORF) consisting 194 amino acids (aa) (Fig. 2C). Northern blot analysis of $polyA^+$ RNA isolated from embryos and third instar larvae confirmed that the cDNAs correspond to full-length transcripts as we can detect *ytr* mRNA bands ranging in size from about 2.0 to 2.2 kb (Fig. 3A).

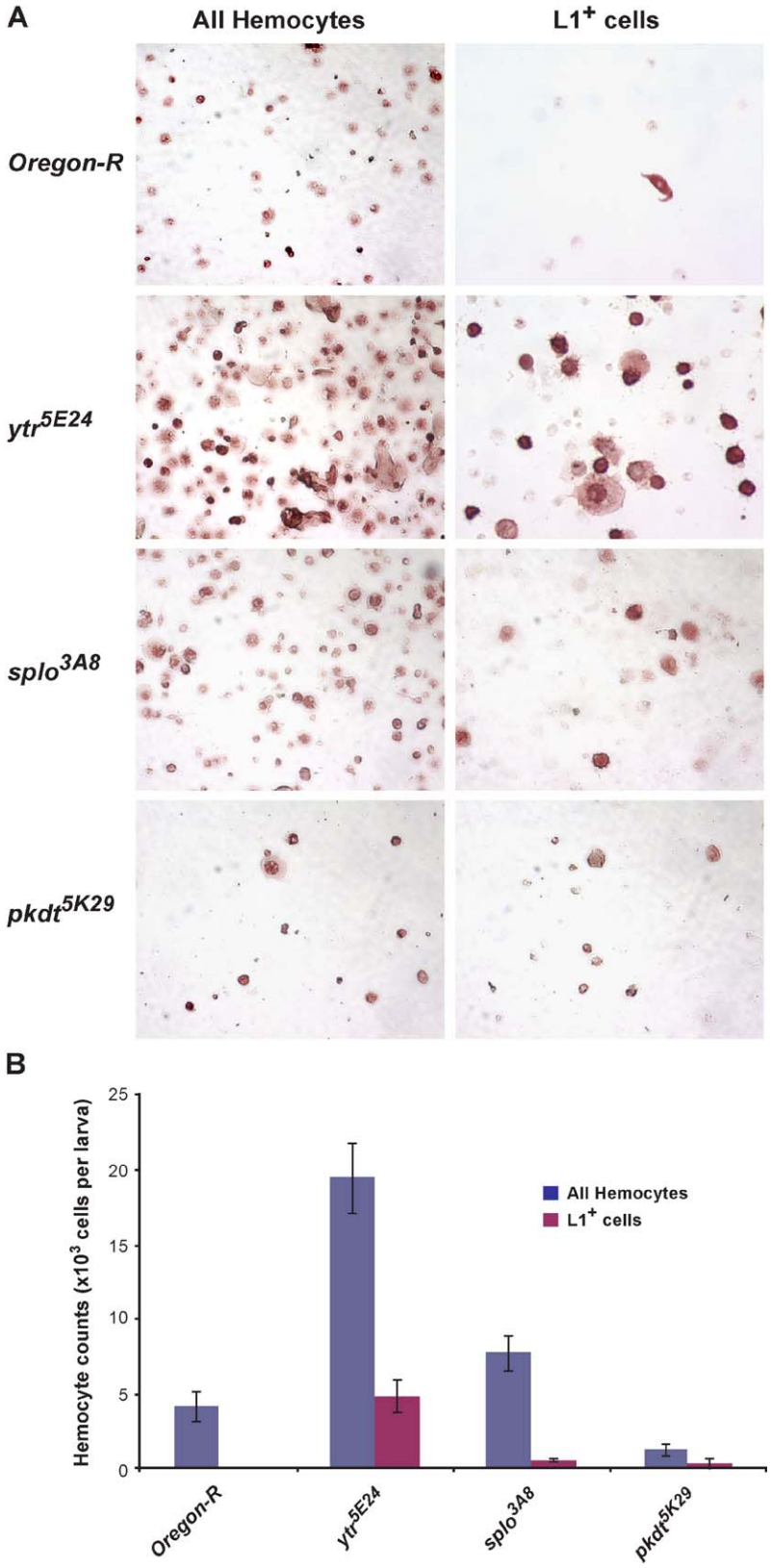

Fig. 1. Aberrant composition of hemocytes in *Drosophila* mutant larvae. (A) Hemolymph from a similar number of third instar wild-type or mutant larvae was collected in the same final volume of buffer and processed for immunostaining using the pan-hemocyte monoclonal antibody H2 and the lamellocyte-specific monoclonal antibody L1 (see Materials and methods for details). (B) Cell counts per mutant or wild-type larva are plotted for all hemocytes (gray bars) and $L1^+$ cells (red bars). Cell counts were calculated as described in Materials and methods.

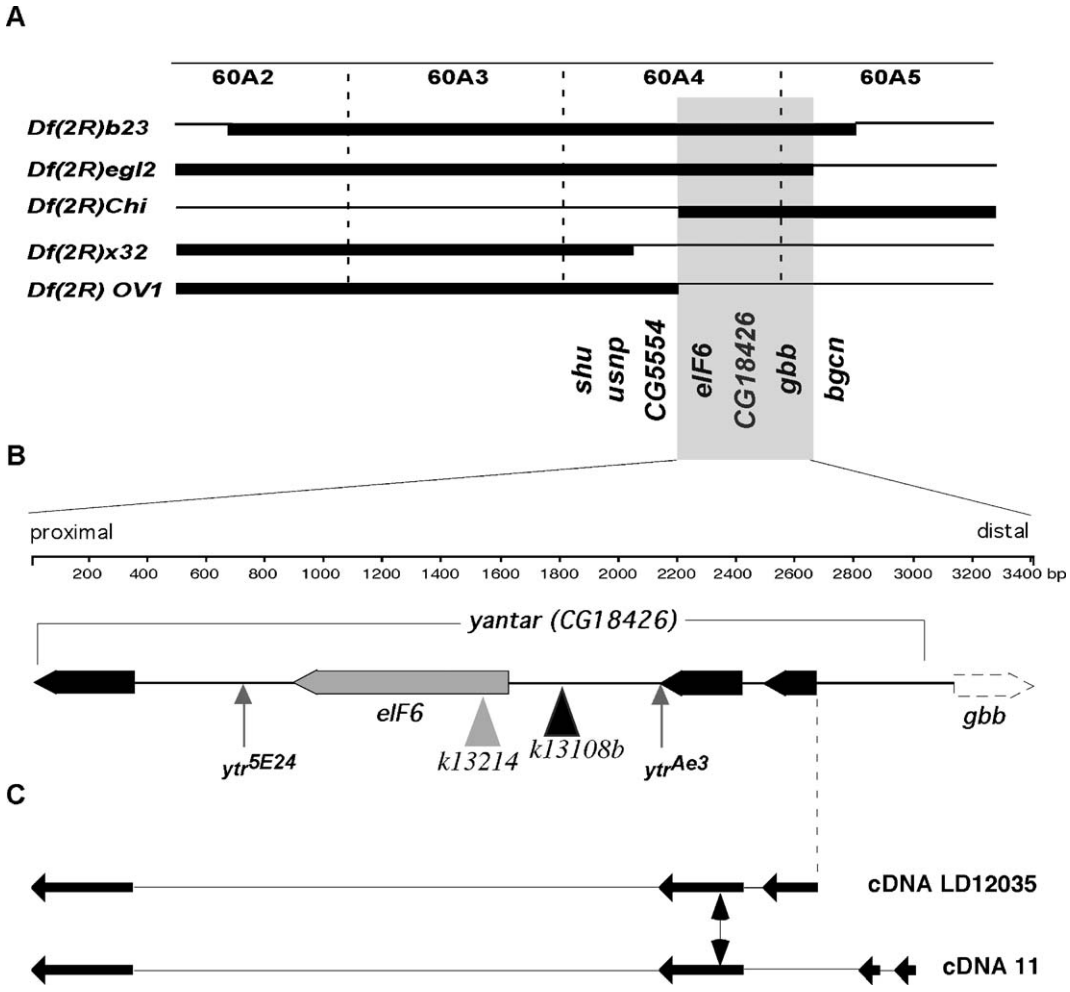

Fig. 2. Genetic map of the 60A chromosomal region in *D. melanogaster*. (A) The thick black line indicates the extent of the deletion in each deficiency. Relevant genes located in the genetic interval of interest are indicated. (B) Schematic representation of the *yantar* locus: A scale [in base pairs (bp)] is shown above the map: the O position was arbitrarily chosen to correspond to the end of the *ytr* gene. The three black arrowed boxes (corresponding *ytr* to the gene) and the gray arrowed box (*eIF6*) are drawn with their relative orientation pointing to the centromeric region of the right arm of chromosome II. Insertion sites for transposons *P-lacW*^{k13214} and *P-lacW*^{k13108b} are indicated with gray and black arrowheads, respectively. Sites where point mutations occur in *ytr*^{5E24} and *ytr*$^{Ae-3}$ are indicated with arrows (see Results for details). (C) Schematic representation of two *ytr* cDNA clones that differ in their 5′ untranslated region but encode a similar ORF. The position for the ATG initiation codon is indicated with vertical, double-headed arrow.

We next examined *ytr* mRNA expression in the different *ytr* alleles. Expression of wild-type size *ytr* mRNA is severely affected in all *ytr* alleles. Either there is a lack of detectable transcripts (as in *ytr*^{k13108b} and its imprecise excision lines) or there is a marked reduction in expression coupled with aberrant migration of *ytr* mRNA (*ytr*^{5E24} and *ytr*$^{Ae-3}$) (Figs. 3A and B). Sequencing of the genomic region in the *ytr*^{5E24} mutant revealed a single nucleotide change (T to A) in the third intron of *ytr* compared to Oregon-R DNA. This change is unlikely to be a natural polymorphism, as it was not observed in the EMS mutant *pkdt*^{5K29} that shares the same genetic background as *ytr*^{5E24}. Interestingly, this mutation also causes a reduction in *eIF6* transcripts (Fig. 3B), possibly by disrupting a regulatory site shared by the two genes. DNA sequencing of the *ytr* genomic sequence of *ytr*$^{Ae-3}$ revealed a single nucleotide (G to A) that destroys the splice donor site in the second intron and prevents proper splicing between the second and third exons. Examination of the sequence just downstream of the mutation shows that there is an in-frame termination codon (TGA) which, if used, would lead to the expression of a truncated Ytr protein (Fig. 2C). This mutation had no affect on the level of *eIF6* transcripts (data not shown).

ytr mRNA is dramatically enriched in larval hematopoietic tissues

ytr mRNA has a dynamic pattern of expression during embryogenesis. It is maternally contributed, and zygotic expression is first detected in invagination furrows and in ventral and head mesoderm. At later stage, it is predominantly detected in the developing neuronal system. At the end of embryogenesis, expression is also found in the area of the presumptive lymph glands and in embryonic hemo-

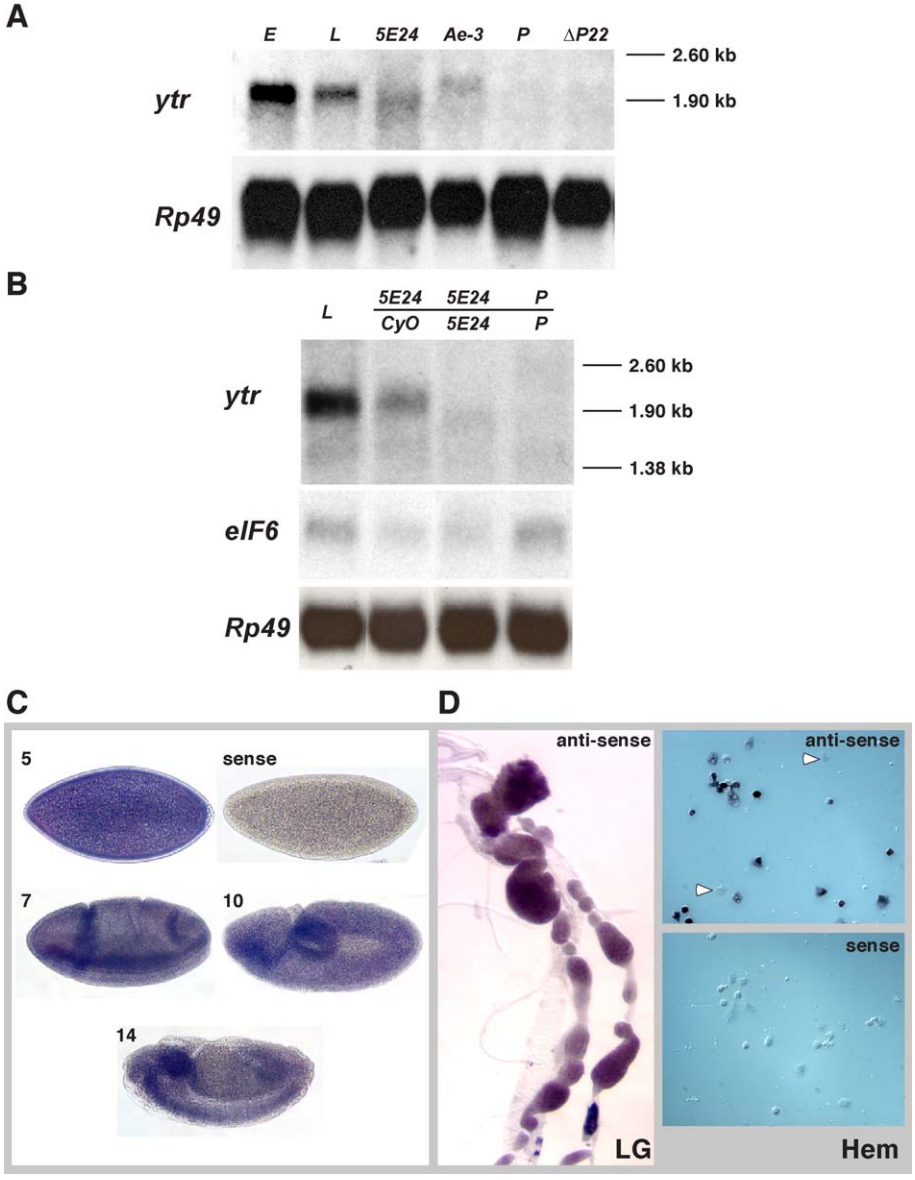

Fig. 3. ytr mRNA expression is affected in the different *ytr* alleles. (A) Poly A^+ mRNA from wild-type embryos (E) or third instar larvae (L) and *ytr* mutant alleles (*5E24*, *Ae-3*, $P^{k13108b}$ (*P*), *ΔP22*) was hybridized with a *ytr* cDNA probe. Migration and steady-state amount of the 2.0- to 2.2-kb *ytr* mRNA are affected in *5E24* and *Ae-3*. Residual or no *ytr* transcripts are detected in the other alleles. (B) Analysis of *ytr* and *eIF6* transcripts in ytr^{5E24} mutant. Steady-state amount of *ytr* mRNA is reduced in heterozygous ytr^{5E24} flies and nearly abolished in ytr^{5E24} homozygous, third instar larvae (note the aberrant migration of residual signal). Detection of the steady-state mRNA levels for *eIF6* indicates that they are equally reduced in heterozygous and homozygous ytr^{5E24} larvae. Molecular standards for RNA size and loading controls (*Rp49*) are included for both panels. In situ hybridization with *ytr* antisense RNA probe on embryo (C) and dissected lymph glands (LG) and circulating hemocytes (Hem) from late third instar larvae (×40 magnification) (D). *ytr* Is expressed in the majority of hemocytes, although single hemocytes consistently fail to show *ytr* expression (black arrow). A negative control *ytr* sense probe shows no hybridization signal in hemocytes.

cytes (Fig. 3C and data not shown). RNA in situ hybridization of larval tissues indicates that *ytr* is strongly expressed in the lymph glands and a majority of peripheral hemocytes (Fig. 3D). *ytr* mRNA is also expressed in imaginal discs, albeit at much lower levels (data not shown). We failed to detect *ytr* expression in other larval tissues. In situ analysis on adult ovaries shows abundant *ytr* mRNA in the nurse cells until stage 10 after which high levels are found in the oocyte (R. Wynn, unpublished).

ytr Encodes a highly conserved arginine-rich protein that predominantly localizes to the nucleus

Based on sequence homologies performed with the conceptual Ytr protein sequence, we have arbitrarily divided the *Drosophila* Ytr protein in four separate domains (Fig. 4A). In addition, these searches revealed that Ytr is highly conserved in fission yeast, *C. elegans*, *Arabidopsis*, and vertebrates (Fig. 4B). Unfortunately, there is no or little

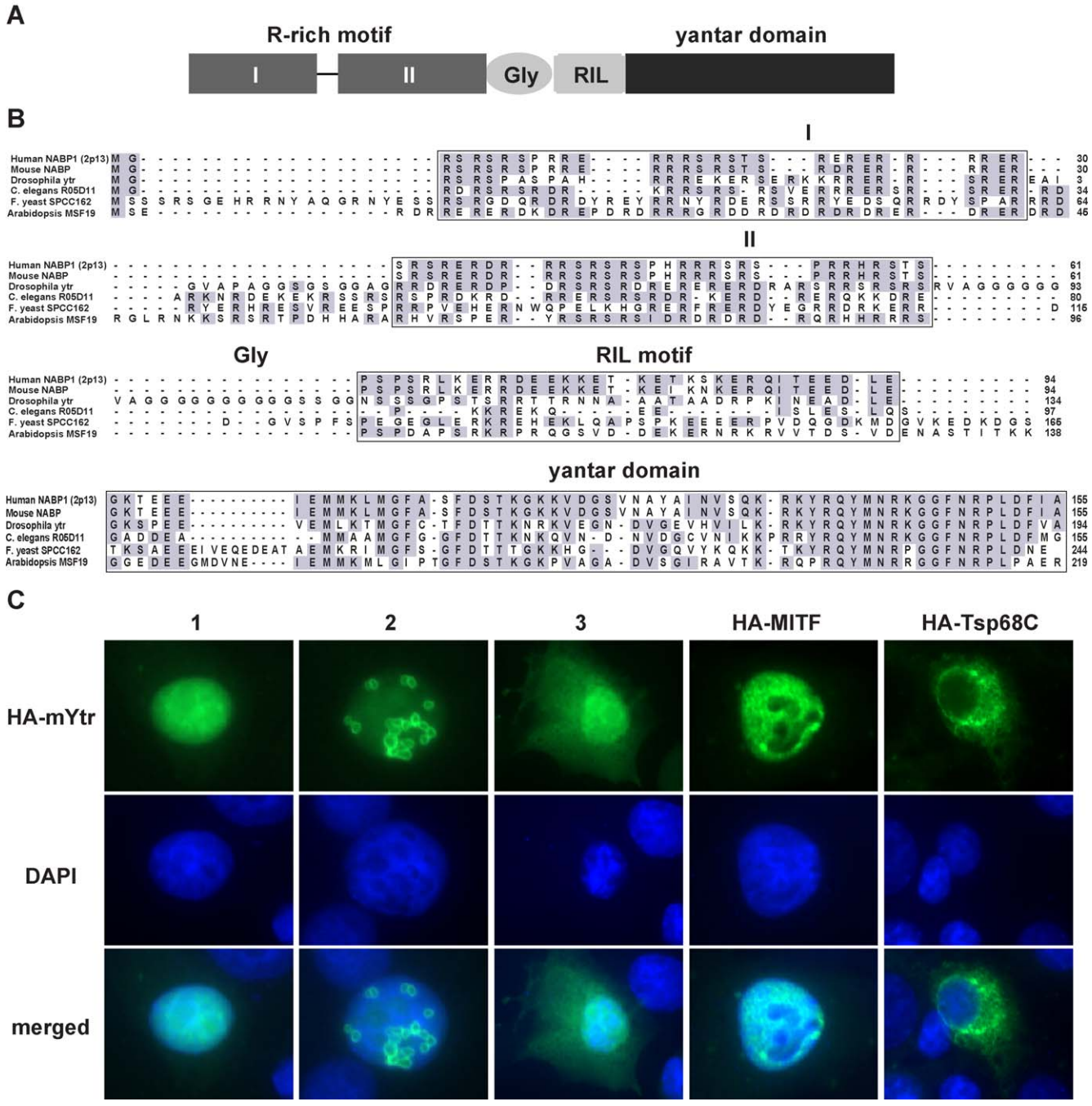

Fig. 4. Schematic of the Ytr protein and sequence comparison. (A) Several putative domains (based on homology searches) were assigned to the Ytr protein: an N-terminal, R-rich motif (I and II), a short glycine repeat (Gly), an unknown motif with conserved Arg, Ile, and Leu residues (RIL motif) and a unique C-terminal domain (*ytr* domain). (B) Sequence alignment of the various domains of *Drosophila* Ytr with orthologs from human, mouse, *C. elegans*, yeast, and *Arabidopsis*. Conserved domains are framed and shading highlights conserved amino acid residues. (C) Subcellular localization of HA-mYtr protein in NIH 3T3 cells: (1): defuse nuclear pattern, (2) punctate nuclear pattern, (3) nuclear and weak cytoplasmic distribution (3). HA-MITF and HA-Tsp68C: control transfections in NIH 3T3 confirm proper localization of the HA-MITF and HA-Tsp68C proteins to the nucleus and cytoplasm, respectively. In all panels, the nucleus is visualized after DAPI staining, and the protein of interest is detected with anti HA-antibody labeled with fluorescein (see Materials and methods).

information to suggest a putative function of Ytr in these various organisms. The N-terminal half of the protein comprises two blocks of charged or serine residues consisting repeated Arg (30% of all residues in the sequence), Ser (8.5%), Asp (5%), and/or Glu (10%) amino acids. This region shows significant homology (40–50%) to domains found in several SR-splicing factors, including U1-70K snRNP protein, SC35, U2AF, as well as RER- and RD-proteins. These repeats have been proposed to mediate direct RNA interaction as well as protein–protein interac-

tion among different SR-proteins (Patel, 1999; Wu and Maniatis, 1993). The Arg-rich repeats are followed by a polyGly-rich linker which is unique to the fly protein and may provide a flexible hinge that precedes a short stretch of amino acids (referred by us as the RIL motif) found in a number of serine/threonine kinases and containing the highly conserved Arg, Ile, and Leu residues. Finally, the C-terminus end of Ytr shows the highest degree of conservation among the various orthologs (Fig. 4B) but shares no significant homology to any other domain in the database. Its function is unknown.

To examine the localization of the Ytr protein, we expressed the mouse Ytr protein tagged with an HA epitope at its N-terminus in NIH 3T3 fibroblasts or COS7 cells. We observed an identical pattern of subcellular localization in both cell types (Fig. 4C and data not shown). Interestingly, we could distinguish three patterns of protein distribution. Consistent with the noted homology to SR-splicing factors, HA-mYtr either localized in a diffuse pattern in the nucleus of transfected fibroblasts (Fig. 4C, 1) or was uniformly distributed between the cytoplasm and nucleus (Fig. 4C, 3). Importantly, in about 10% of the transfected cells, we

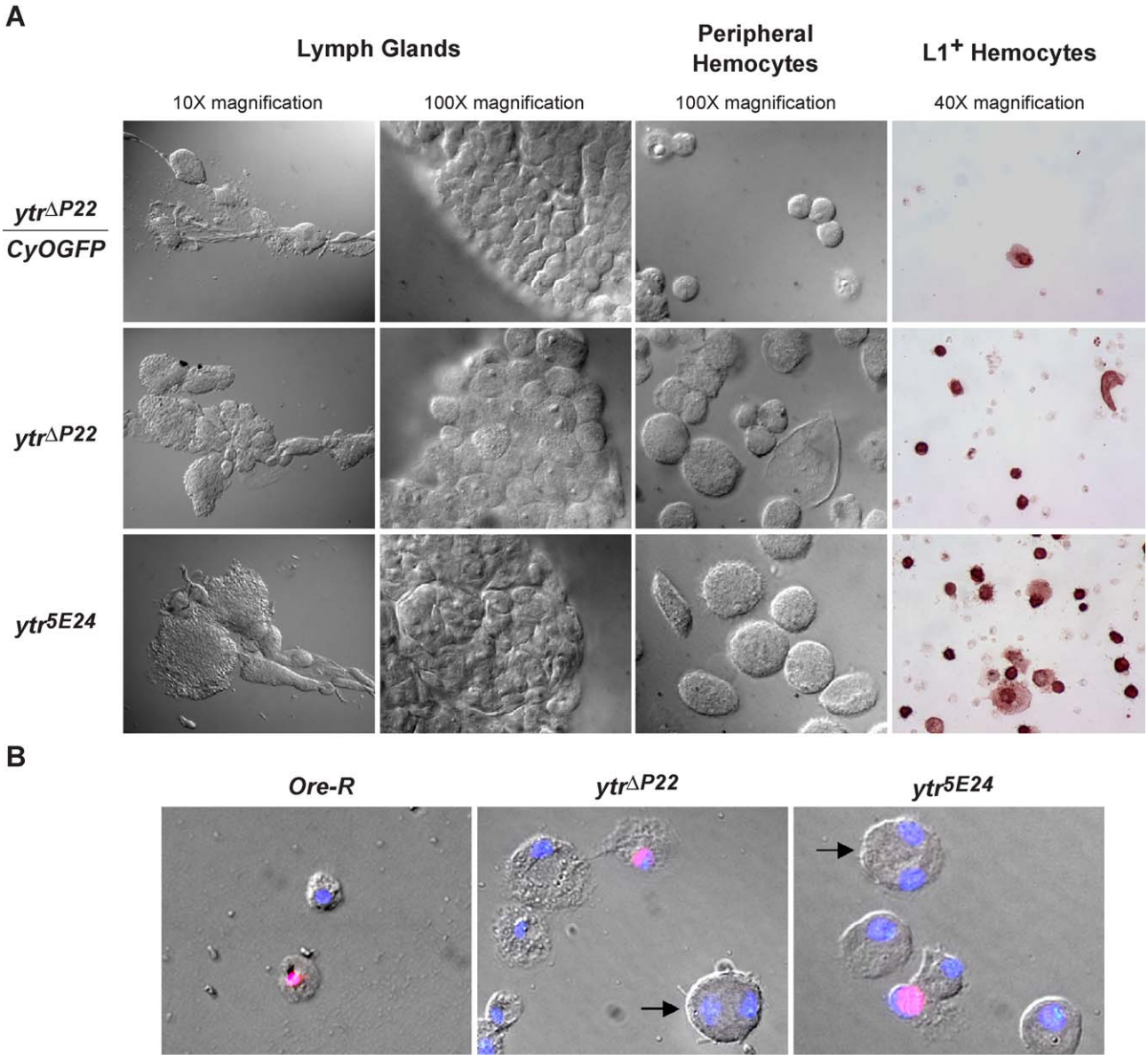

Fig. 5. Hemocytes in different *ytr* alleles. (A) Analysis of lymph gland and circulating hemocytes in larvae-bearing homozygous mutations in *ytr* (*5E24* and *ΔP22*) was examined by Nomarski microscopy under the indicated magnification, and immunostaining with L1 antibody was performed on circulating hemocytes to reveal lamellocytes. (B) A population of large round hemocytes (black arrows) from *ytr* mutant larvae often contains two nuclei (DAPI epifluorescence, blue). Binucleated hemocytes from mutant larvae are not actively dividing as evidenced by the lack of antiphosphohistone H3 immunoreactivity (purple, ×120 magnification).

observed a punctate distribution of the protein (spherical doughnuts) in the nucleus (Fig. 4C, 2). These discrete puncta often localized to areas of less condensed chromatin. Control transfections with HA-tag MITF transcription factor (King et al., 1999) and HA-tag tetraspanin protein Tsp68C (S.A. Sinenko and B. Mathey-Prevot, unpublished) expression plasmids confirmed that under our experimental conditions, the two proteins localized to their proper compartment (nuclear and cytoplasmic, respectively).

Loss of Ytr function results in the detection of an altered population of Lz/L1 double-positive hemocytes and binucleated hemocytes

Null and hypomorphic alleles of *ytr* cause a marked enlargement of the first lobes of the lymph gland (LG), which occasionally contain melanized hemocytes (Fig. 5A). In addition, hemocytes in the mutant LG are larger ($ytr^{\Delta P22}$) and more heterogeneous in size and shape (ytr^{5E24}) than those found in wild-type LG. Analysis of the circulating hemocytes revealed the presence of numerous big round cells that are normally absent in wild-type and *ytr* heterozygous larvae (Fig. 5A, data not shown). As their appearance was somewhat reminiscent of lamellocytes, mutant circulating hemocytes were stained for the specific marker L1 expressed by wild-type lamellocytes. As already observed for ytr^{5E24} (Fig. 1), there was a substantial increase in the percentage of circulating $L1^+$ cells in this and other *ytr* mutants, ranging from 10% to 35% of total hemocytes (Figs. 5A and 6A). Unlike the restricted expression of the L1 antigen to circulating lamellocytes in wild-type hemolymph, this antigen was detected in *ytr* mutant hemocytes that showed distinct morphology from that of typical lamellocytes. In particular, a number of small round *ytr* mutant hemocytes were highly L1 positive (Fig. 5A). In addition, many of the large round mutant hemocytes in lymph glands and in circulation (up to 10% of all hemocytes) contained two nuclei (Fig. 5B). These cells, however, do not express the phosphorylated form of histone H3 (Fig. 5B), indicating that they are not dividing cells but rather exhibit a defect in cytokinesis.

To characterize further the differentiation defect in *ytr* mutant hemocytes, we monitored the expression of the crystal cell marker Lz in these cells, both by immunocytochemistry (Figs. 6B and C) and using the *lz*-Gal4 enhancer trap line (Figs. 6D and E). Normally, Lz is highly expressed in mature crystal cells and to a lesser extent in a rare population of small, circulating hemocytes (presumably crystal cell precursors). Although the production of mature crystal cells was not measurably affected in *ytr* mutant hemolymph, there was an increase in lymph gland and circulating Lz^+ hemocytes. These cells were heterogeneous in size and lacked the characteristic paracrystalline inclusions (Figs. 6D and E). The largest increase was observed in ytr^{5E24} larval hemolymph. There was a concomitant enrichment of Lz^+ cells in the first lobe of the LG of ytr^{5E24} mutant larvae (as visualized with the *lz* enhancer trap *lz*-Gal4 and UAS-GFP; Fig. 6B). Interestingly, there was a mild elevation of Lz^+ cells in the LG of male ytr^{5E24} heterozygous larvae, indicative perhaps of a genetic interaction between *ytr* and the hypomorphic *lz* allele of this enhancer trap line (Fig. 6D).

A closer examination of the $L1^+$ and Lz^+ hemocytes in *ytr* mutant revealed that some cells shared a common morphology. To determine whether these cells might coexpress both antigens, the *lz*-Gal4 enhancer trap was used to visualize Lz^+ hemocytes in wild-type or mutant hemolymph (through expression of GFP), and we counterstained the same cells with the L1 antibody (Fig. 6D). As expected, the strongly GFP-positive (GFP^+) cells in wild-type hemolymph are either crystal cells (white arrow in Fig. 6C) or small round cells (presumably crystal cell precursors). Importantly, these cells do not express the L1 antigen. On rare occasion, we noticed dimly GFP^+ cells that also expressed L1 (red arrow). These cells differ slightly in morphology from mature lamellocytes that are invariably GFP-negative (black arrow, Fig. 6D). Whether coexpression of the two antigens in these cells defines a distinct or transient population is not known. Regardless, we found up to 20% of $L1^+$ hemocytes that expressed both antigens in ytr^{5E24} mutant hemolymph (red arrows, Fig. 6C), consistent with the expansion of a rare population of hemocytes or with the overproliferation of bi- or multipotential progenitors in ytr^{5E24} mutants.

Mouse Ytr corrects ytr mutant hemocytes and leads to full rescue

We next selected a Gal4 enhancer trap $P[GawB]^{5015}$ that was described in FlyBase as an LG-specific line. Using the GFP reporter gene, we confirmed that this line drove expression in the LG and in about 50% of circulating hemocytes of ytr^{5E24} mutants (Fig. 7A). Interestingly, and consistent with an elevation of precursor cells in *ytr* mutants (normally found in the LG), there was no or little GFP expression in *ytr* heterozygous or in wild-type circulating hemocytes (Fig. 7A and data not shown). In addition, GFP was expressed in the salivary glands and ring gland, two tissues where we failed to detect *ytr* expression (data not shown). Ectopic expression of *Drosophila* (d)-Ytr or mouse (m)-Ytr mediated by $P[GawB]^{5015}$ rescued the hematopoietic phenotype in both ytr^{5E24}/ytr^{5E24} and ytr^{5E24}/ytr^{AP22} mutants (Fig. 7A and data not shown). Interestingly, m-Ytr was more efficient at rescuing the phenotype, although this difference may reflect different levels in protein expression. Despite having normal hemocytes and lymph glands, mutant larvae that expressed m-Ytr (or d-Ytr) still died at the pupal stage, suggesting that Ytr function is required in other tissues. To confirm this interpretation, m-Ytr was expressed ubiquitously in mutants through the use of *daughterless* (*da*)-Gal4 driver. The hematopoietic defects and lethality were completely rescued in *ytr* mutants after *da*-Gal4 mediated expression of m-Ytr (Fig. 7B). The emerging adults showed no obvious phenotype and were fertile (data not shown).

Discussion

Three novel mutations affect normal hemocyte development

The transcription factors, Srp, Lz, Ush, and Gcm, have all been implicated in the specification and function of plasmatocytes and crystal cells (for review, see Evans et al. 2003). However, little is known about the origin and differentiation requirements of the lamellocyte lineage. Mutations in the Jak-kinase Hopscotch (*hop*$^{Tum\text{-}l}$, *hop*^{T42}), in the Toll/cactus pathway (*Toll*^{10B} and *cact*$^{E8/D13}$), as well as in the putative cell adhesion protein *l(3)mbn-1*, in ribosomal protein *RpS6*^{air8}, or in the nucleosome remodeling factor (*NURF301*^{2}) lead to overproliferation of larval hemocytes accompanied by a large increase in circulating lamellocytes in mutant larvae (Badenhorst et al., 2002; Harrison et al., 1995; Konrad et al., 1994; Qiu et al., 1998; Watson et al., 1992). As these mutations appear to act in a cell autonomous fashion, these genes or pathways have been linked to the regulation of hemocyte development. To gain additional information on genes that affect the lamellocyte lineage, we screened a collection of EMS mutants and identified several complementation groups, which when homozygous, led to the appearance of melanotic masses in larvae. Three of these mutants—*yantar*, *polka dots*, and *splotchy*—were further selected as they exhibited profound anomalies in circulating larval hemocytes. There was a large increase in the relative number of lamellocytes or L1^{+} cells in each mutant, and the number of circulating hemocytes was significantly increased in *ytr*^{5E24} mutants. Although detection of melanotic masses correlated with altered hemocyte differentiation and overrepresentation of L1^{+} cells, it did not always result in hemocyte overproliferation as exemplified by the drastic reduction in circulating hemocytes in *pkdt*^{5K29} mutants.

Ytr is a conserved arginine-rich protein with nuclear localization

Our genetic mapping and molecular analyses indicate that *ytr* corresponds to *CG18426* located in 60A. Although we have focused on the role of *ytr* in hematopoiesis, *ytr* loss of function also results in a marked reduction in imaginal disc size and in a mild loss of actin organization in disc cells (data not shown). The relative enrichment of *ytr* mRNA in developing tissues (embryonic head and ventral mesoderm, developing gut, embryonic brain, and lymph glands) and in actively proliferating tissues (hemocytes and imaginal discs) coupled with the range of defects observed in *ytr* mutants suggest that *ytr* plays a role in regulating growth and differentiation.

Ytr protein shows high evolutionary conservation, and orthologs can be identified in different phylogenic classes of the metazoa. Aside from one report on the ectopic expression of human *ytr* mRNA in a human lymphocytic cell line as a result of a viral integration (Nakamura et al., 1994), nothing is known about the Ytr proteins in other species. Based on the homology of the R-rich domains in the N-terminal region of Ytr with RS domains found in several SR-splicing factors as well as in RE- and RD-proteins, we speculate that Ytr is involved in nucleic acid binding, either directly or indirectly. Although the two R-rich domains in Ytr lack the canonical RNA-recognition motif (RRM) thought to mediate RNA binding, viral proteins with similar R-rich motifs or RS, RD, and RE dipeptide repeats have been described to be directly involved in RNA recognition and splicing activation (Patel, 1999; Shen et al., 2004). RS domains have also been implicated in protein–protein interaction among different SR-splicing factors, and their phosphorylation have been proposed to promote nuclear import, nuclear retention, as well as activation of these proteins and their complexes (Cazalla et al., 2002; Wu and Maniatis, 1993). Although we have no biochemical proof that Ytr binds RNA (or DNA), its dynamic pattern of subcellular localization and punctate nuclear distribution is reminiscent of that of many SR and arginine-rich proteins (de Graaf et al., 2004; van der Houven van Oordt et al., 2000). Consistent with this prediction is the fact that several related RNA-binding proteins and splicing factors have been linked to growth and differentiation. For instance, the *Drosophila* Musashi RNA-binding protein functions in asymmetric cell division downstream of Notch signaling by regulating the translation of the transcription factor TTK69 (Okano et al., 2002) and alternative splicing by SR proteins have been shown to play a role in human T cell development (Wang et al., 2001). Alternatively, the potential homology of the Ytr N-terminal half with the Acinus protein might suggest that Ytr, like Acinus, has chromatin remodeling activity. Interestingly, Acinus is involved in caspase-3-dependent apo-

Fig. 6. Accumulation of Lz^{+} and L1^{+} hemocytes in *ytr*^{5E24} mutants. (A) Total peripheral hemocytes were counted as described in Materials and methods. Average total counts (blue bars) are reported for a single larva of the indicated genotype. (B) Hemocytes were immunostained with antibodies directed against the L1 antigen (Mab L1) and Lz protein (Mab α-Lz). Positive cells for each antigen were counted, and counts were plotted as cells/larva (see Materials and methods): L1^{+} hemocytes (red bars) and Lz^{+} hemocytes (green bars). (C). Representative panels of wild-type and *ytr* mutant peripheral hemocytes immunostained with α-Lz Mab. (D) Lz^{+} cells (green) in anterior lobes of larval lymph glands of the indicated genotypes were visualized with the *lz*-Gal4, UAS-GFP reporter line (×20 magnification). (E) Hemocytes were immunostained with Mab L1 and visualized under Nomarski or epifluorescence (GFP) microscopy. In wild-type, third instar larvae, the L1 antigen is restricted to lamellocytes (black arrows) among circulating hemocytes, while Lz (GFP^{+}) is strongly expressed in crystal cells (white arrows) and their precursors. Rare Lz^{+}/L1^{+} double-positive cells (orange arrow) are present in normal larval hemolymph. High numbers of L1^{+} (black arrows), Lz^{+} (white arrows) as well as Lz^{+}/L1^{+} double-positive cells (orange arrows) circulate in *ytr*^{5E24} mutant hemocytes (×80 magnification). Third instar larvae from the *lz*-Gal4, *UAS-GFP* and *lz*-Gal4, *UAS-GFP*; *Bc/CyOGFP* stocks were used as control for wild-type hemolymph.

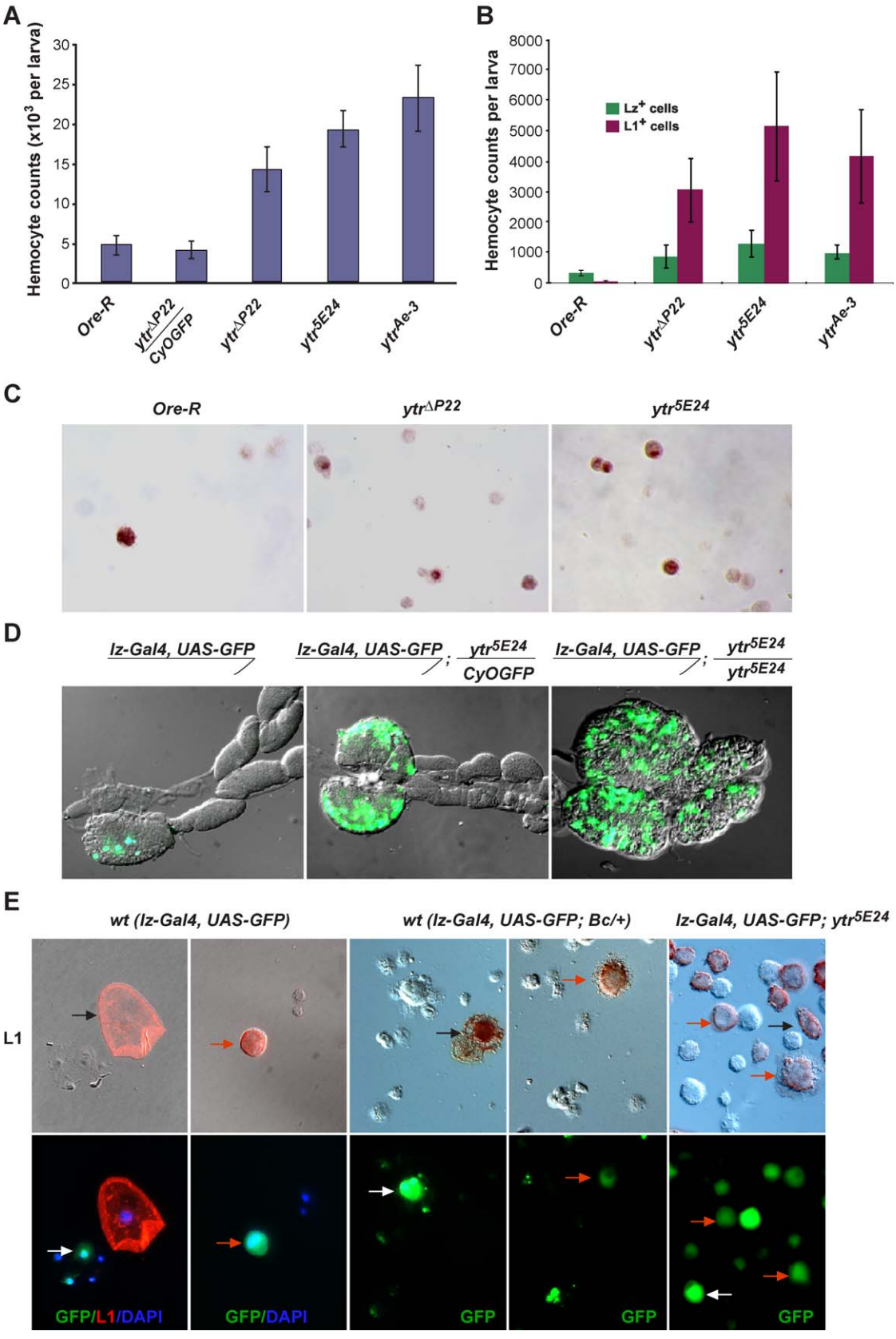
A
Hemocyte counts (x10^3 per larva)
30
25
20
15
10
5
0
Ore-R
ytrΔP22/CyOGFP
ytrΔP22
ytr5E24
ytrAe-3
B
Hemocyte counts per larva
8000
7000
6000
5000
4000
3000
2000
1000
0
Lz+ cells
L1+ cells
Ore-R
ytrΔP22
ytr5E24
ytrAe-3
C
Ore-R
ytrΔP22
ytr5E24
D
lz-Gal4, UAS-GFP
lz-Gal4, UAS-GFP; ytr5E24/CyOGFP
lz-Gal4, UAS-GFP; ytr5E24/ytr5E24
E
wt (lz-Gal4, UAS-GFP)
wt (lz-Gal4, UAS-GFP; Bc/+)
lz-Gal4, UAS-GFP; ytr5E24
L1
GFP/L1/DAPI
GFP/DAPI
GFP
GFP
GFP

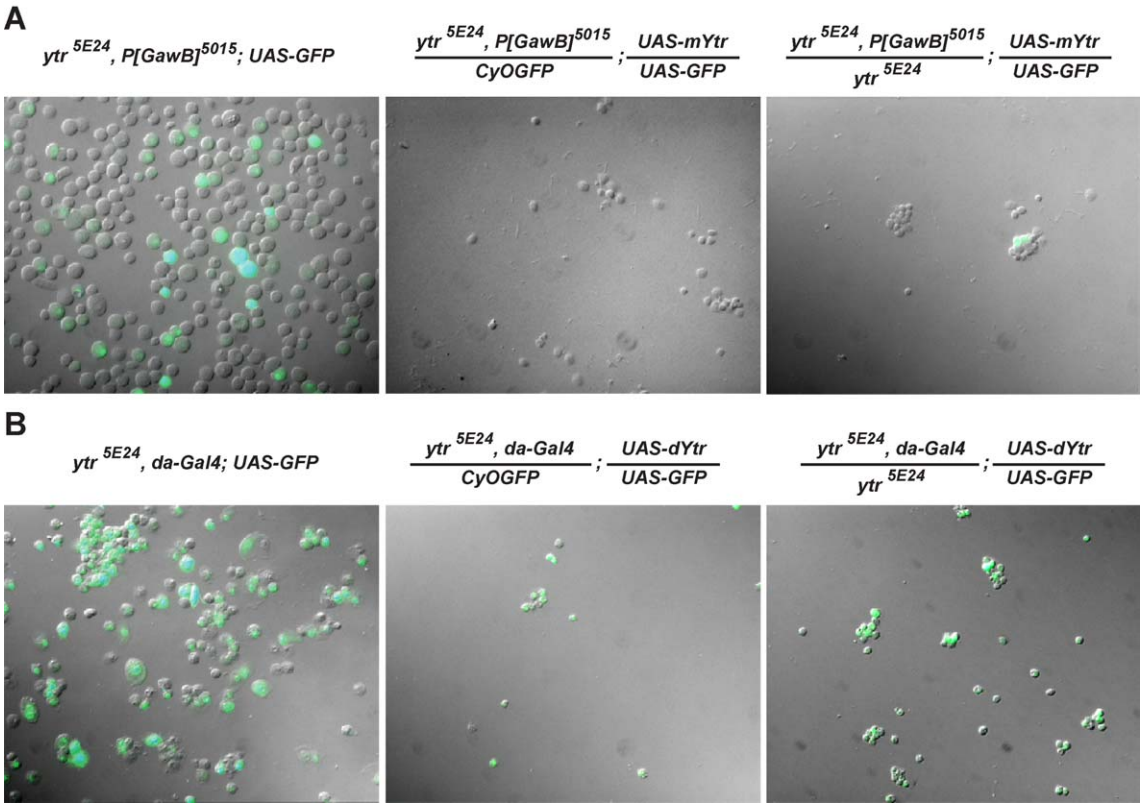

Fig. 7. Blood rescue after ectopic expression of m-Ytr in hemocytes. (A) P[GawB]^{5015}- and (B) *da*-Gal4-mediated GFP expression in circulating hemocytes from *ytr*^{5E24} homozygous and heterozygous larvae before and after rescue with UAS-mYtr or UAS-dYtr [merged Nomarski and GFP (green) images, ×20 magnification].

ptotic chromosome condensation and is required for erythroblasts maturation and differentiation of monocytes to macrophages in mammals (Sordet et al., 2002). Regardless of the exact mechanism, we propose that the N-terminal region of Ytr is important to promote its nuclear retention where this protein can function in cell differentiation or proliferation by regulating posttranscriptional events through RNA binding or RNA processing, or by participating in DNA remodeling.

The ytr^{5E24} allele is a complex mutation

We do not fully understand how the mutation in *ytr*^{5E24} results in drastically reduced levels of aberrantly sized *ytr* mRNA transcripts. One possible explanation is that the mutation creates a $(GA)_3$ site that could recruit GAFs chromatin remodeling factors known to render DNA sequences more accessible to various nucleases and other factors (Henikoff and Vermaak, 2000; Leibovitch et al., 2002). Recruitment of GAFs to the *ytr* locus might alter the surrounding chromatin structure, consistent with our observation that *eIF6* expression is reduced in *ytr*^{5E24}, although it is completely unaffected in other *ytr* alleles. Interestingly, we have found that a short DNA fragment spanning the mutation was difficult to amplify in a PCR reaction. Lastly, in addition to the aberrantly sized transcripts that lacked the third exon, we have recovered hybrid transcripts in *ytr*^{5E24} mutants that contained *ytr* 5′ exons fused to a sequence from *eIF6* (data not shown). This data confirm that the mutation in *ytr*^{5E24} is complex and, through its additional effect on *eIF6* expression, may explain why the hematopoietic phenotype observed with this allele is quite severe.

Ytr function is required for proper hemocyte differentiation

All *ytr* mutations result in hematopoietic defects in late third instar larvae characterized by the presence of a large number of $L1^+$ and Lz^+ circulating hemocytes. In wild-type hemolymph, the L1 antigen is a specific marker of mature lamellocytes (Asha et al., 2003). Wild-type lamellocytes adopt a variety of cell sizes and shapes in vivo which may reflect transitional stages in cell maturation. The morphology and size of $L1^+$ cells circulating in *ytr* mutant hemolymph are even more diverse. Aside from typical lamellocytes, there is an abundance of round cells of heterogeneous sizes, including cells that are hard to distinguish from plasmatocytes based on morphology alone. Plasmatocytes, however, do not express the L1 antigen, leaving open the possibility that these $L1^+$ cells may represent lamellocyte precursor cells. Confirmation of this hypothesis will require the use of additional markers of the lamellocyte lineage. Another possibility is that

the *ytr* mutation leads to the derepression and ectopic expression of the L1 antigen in some hemocytes. This explanation is made less likely by our observation that many of the $L1^+$ cells in the ytr^{5E24} mutant also express the Lz marker while being morphologically distinct from crystal cells and their precursors. Furthermore, we can detect very rare cells in wild-type hemolymph that similarly coexpress the two markers. We therefore favor the idea that such double-positive cells represent early progenitors of either the lamellocytic lineage or of a normally rare subset of hemocytes distinct from lamellocytes and that these cells are specifically expanded in *ytr* mutants. Consistent with this notion is our observation that Gal4 expression in the enhancer trap gene $P[GawB]^{5015}$ is normally restricted to rare hemocytes in the LG but is dramatically upregulated in all lobes of the LG and in circulating hemocytes in ytr^{5E24} mutants. Based on these observations, we propose that the loss of Ytr function leads to an expansion and block or delay in maturation of hemocyte precursors. This defect was readily reversed after ectopic expression of wild-type fly and mouse Ytr proteins in mutant hemocytes, a strong indication of the evolutionary conservation and importance of *ytr* function in *Drosophila* hematopoiesis.

Acknowledgments

We thank Bernard Callus, Maja-Ulla Petersen, Hans Widlund, and members of the Perrimon laboratory for helpful discussions on this project. We thank the reviewers for their critical reading and helpful suggestions on the manuscript. We are grateful to Eva Kurucz, Peter Vilmos, Istvan Nagy, Robert Markus, Yves Carton, Imre Ocsovszki, Dan Hultmark, and Elisabeth Gateff for valuable expertise in hemocyte characterization and for making available the anti-H2 and anti-L1 monoclonal antibodies. We thank Drs. Hand Widlund and David Fisher for providing the HA-tag MITF cDNA expression plasmid, and we are grateful to Drs. Utpal Banerjee, Seung-Hye Jung, and Nancy Fossett for providing Lz- and Ush-specific antibodies. We are grateful for the expertise of L. Hrdlicka and C. Villalta in performing embryo injections. We acknowledge the Bloomington Stock Center for providing us with numerous fly stocks. This work was supported in part by grant R01 HL62434 and the Claudia Adams Barr Program in Cancer Research (B.M.-P.), the National Science Foundation IBN-9205808 (K.W.), and the Hungarian Science Foundation OTKA Grant Nos. T035074 and T035249 (I.A.).

References

Adams, M.D., Celniker, S.E., Holt, R.A., Evans, C.A., Gocayne, J.D., Amanatides, P.G., Scherer, S.E., Li, P.W., Hoskins, R.A., Galle, R.F., George, R.A., Lewis, S.E., Richards, S., Ashburner, M., Henderson, S.N., Sutton, G.G., Wortman, J.R., Yandell, M.D., Zhang, Q., Chen, L.X., Brandon, R.C., Rogers, Y.H., Blazej, R.G., Champe, M., Pfeiffer, B.D., Wan, K.H., Doyle, C., Baxter, E.G., Helt, G., Nelson, C.R., Gabor, G.L., Abril, J.F., Agbayani, A., An, H.J., Andrews-Pfannkoch, C., Baldwin, D., Ballew, R.M., Basu, A., Baxendale, J., Bayraktaroglu, L., Beasley, E.M., Beeson, K.Y., Benos, P.V., Berman, B.P., Bhandari, D., Bolshakov, S., Borkova, D., Botchan, M.R., Bouck, J., Brokstein, P., Brottier, P., Burtis, K.C., Busam, D.A., Butler, H., Cadieu, E., Center, A., Chandra, I., Cherry, J.M., Cawley, S., Dahlke, C., Davenport, L.B., Davies, P., de Pablos, B., Delcher, A., Deng, Z., Mays, A.D., Dew, I., Dietz, S.M., Dodson, K., Doup, L.E., Downes, M., Dugan-Rocha, S., Dunkov, B.C., Dunn, P., Durbin, K.J., Evangelista, C.C., Ferraz, C., Ferriera, S., Fleischmann, W., Fosler, C., Gabrielian, A.E., Garg, N.S., Gelbart, W.M., Glasser, K., Glodek, A., Gong, F., Gorrell, J.H., Gu, Z., Guan, P., Harris, M., Harris, N.L., Harvey, D., Heiman, T.J., Hernandez, J.R., Houck, J., Hostin, D., Houston, K.A., Howland, T.J., Wei, M.H., Ibegwam, C., et al., 2000. The genome sequence of *Drosophila melanogaster*. Science 287, 2185–2195.

Alfonso, T.B., Jones, B.W., 2002. gcm2 Promotes glial cell differentiation and is required with glial cells missing for macrophage development in *Drosophila*. Dev. Biol., vol. 248, pp. 369–383.

Asha, H., Nagy, I., Kovacs, G., Stetson, D., Ando, I., Dearolf, C.R., 2003. Analysis of ras-induced overproliferation in *Drosophila* hemocytes. Genetics 163 (1), 203–215.

Badenhorst, P., Voas, M., Rebay, I., Wu, C., 2002. Biological functions of the ISWI chromatin remodeling complex NURF. Genes Dev. 16, 3186–3198.

Callus, B.A., Mathey-Prevot, B., 2002. SOCS36E, a novel *Drosophila* SOCS protein, suppresses JAK/STAT and EGF-R signalling in the imaginal wing disc. Oncogene 21, 4812–4821.

Cazalla, D., Zhu, J., Manche, L., Huber, E., Krainer, A.R., Caceres, J.F., 2002. Nuclear export and retention signals in the RS domain of SR proteins. Mol. Cell. Biol. 22, 6871–6882.

Cho, N.K., Keyes, L., Johnson, E., Heller, J., Ryner, L., Karim, F., Krasnow, M.A., 2002. Developmental control of blood cell migration by the *Drosophila* VEGF pathway. Cell 108, 865–876.

Dearolf, C.R., 1998. Fruit fly "leukemia". Biochim. Biophys. Acta 1377, M13–M23.

de Graaf, K., Hekerman, P., Spelten, O., Herrmann, A., Packman, L.C., Bussow, K., Muller-Newen, G., Becker, W., 2004. Characterization of cyclin L2, a novel cyclin with an arginine/serine-rich domain: phosphorylation by DYRK1A and colocalization with splicing factors. J. Biol. Chem. 279 (6), 4612–4624.

Duvic, B., Hoffmann, J.A., Meister, M., Royet, J., 2002. Notch signaling controls lineage specification during *Drosophila* larval hematopoiesis. Curr. Biol. 12, 1923–1927.

Evans, C., Hartenstein, V., Banerjee, U., 2003. Thicker than blood: conserved mechanisms in *Drosophila* and vertebrate hematopoiesis. PG-673-90. Dev. Cell 5, 673–690.

Fossett, N., Tevosian, S.G., Gajewski, K., Zhang, Q., Orkin, S.H., Schulz, R.A., 2001. The Friend of GATA proteins U-shaped, FOG-1, and FOG-2 function as negative regulators of blood, heart, and eye development in *Drosophila*. Proc. Natl. Acad. Sci. U. S. A. 98, 7342–7347.

Gateff, E., 1978. Malignant neoplasms of genetic origin in *Drosophila melanogaster*. Science 200, 1448–1459.

Harrison, D.A., Binari, R., Stines Nahreini, T., Gilman, M., Perrimon, N., 1995. Activation of a *Drosophila* janus kinase (JAK) causes hematopoietic neoplasia and developmental defects. EMBO J. 14, 2857–2865.

Henikoff, S., Vermaak, D., 2000. Bugs on drugs go GAGAA. Cell 103, 695–698.

Holz, A., Bossinger, B., Strasser, T., Janning, W., Klapper, R., 2003. The two origins of hemocytes in *Drosophila*. Development 130 (20), 4955–4962.

Huber, W.E., Price, E.R., Widlund, H.R., Du, J., Davis, I.J., Wegner, M., Fisher, D.E., 2003. A tissue-restricted cAMP transcriptional response: SOX10 modulates alpha-melanocyte-stimulating hormone-triggered expression of microphthalmia-associated transcription factor in melanocytes. J. Biol. Chem. 278 (46), 45224–45230.

King, R., Weilbaecher, K.N., McGill, G., Cooley, E., Mihm, M., Fisher,

T., 1999. Microphthalmia transcription factor. A sensitive and specific melanocyte marker for melanoma diagnosis. Am. J. Pathol. 155 (3), 731–738.

Konrad, L., Becker, G., Schmidt, A., Klockner, T., Kaufer-Stillger, G., Dreschers, S., Edstrom, J.E., Gateff, E., 1994. Cloning, structure, cellular localization, and possible function of the tumor suppressor gene lethal(3) malignant blood neoplasm-1 of *Drosophila melanogaster*. Dev. Biol. 163, 98–111.

Kurucz, E., Zettervall, C.J., Sinka, R., Vilmos, P., Pivarcsi, A., Ekengren, S., Hegedus, Z., Ando, I., Hultmark, D., 2003. Hemese, a hemocyte-specific transmembrane protein, affects the cellular immune response in *Drosophila*. Proc. Natl. Acad. Sci. U. S. A. 100, 2622–2627.

Lanot, R., Zachary, D., Holder, F., Meister, M., 2001. Postembryonic hematopoiesis in *Drosophila*. Dev. Biol. 230, 243–257.

Lebestky, T., Chang, T., Hartenstein, V., Banerjee, U., 2000. Specification of *Drosophila* hematopoietic lineage by conserved transcription factors. Science 288, 146–149.

Lebestky, T., Jung, S., Banerjee, U., 2003. A serrate-expressing signaling center controls *Drosophila* hematopoiesis. Genes Dev. 17, 348–353.

Leibovitch, B.A., Lu, Q., Benjamin, L.R., Liu, Y., Gilmour, D.S., Elgin, S.C., 2002. GAGA factor and the TFIID complex collaborate in generating an open chromatin structure at the *Drosophila melanogaster* hsp26 promoter. Mol. Cell. Biol. 22, 6148–6157.

Lukacsovich, T., Asztalos, Z., Juni, N., Awano, W., Yamamoto, D., 1999. The *Drosophila melanogaster* 60A chromosomal division is extremely dense with functional genes: their sequences, genomic organization, and expression. Genomics 57, 43–56.

Luo, H., Rose, P.E., Roberts, T.M., Dearolf, C.R., 2002. The Hopscotch Jak kinase requires the Raf pathway to promote blood cell activation and differentiation in *Drosophila*. Mol. Genet. Genomics 267, 57–63.

Mathey-Prevot, B., Perrimon, N., 1998. Mammalian and *Drosophila* blood: JAK of all trades? Cell 92, 697–700.

Munn, K., Steward, R., 2000. The shut-down gene of *Drosophila melanogaster* encodes a novel FK506-binding protein essential for the formation of germline cysts during oogenesis. Genetics 156, 245–256.

Nakamura, Y., Moriuchi, R., Nakayama, D., Yamashita, I., Higashiyama, Y., Yamamoto, T., Kusano, Y., Hino, S., Miyamoto, T., Katamine, S., 1994. Altered expression of a novel cellular gene as a consequence of integration of human T cell lymphotropic virus type 1. J. Gen. Virol. 75, 2625–2633.

Ohlstein, B., Lavoie, C.A., Vef, O., Gateff, E., McKearin, D.M., 2000. The *Drosophila* cystoblast differentiation factor, benign gonial cell neoplasm, is related to DExH-box proteins and interacts genetically with bag-of-marbles. Genetics 155, 1809–1819.

Okano, H., Imai, T., Okabe, M., 2002. Musashi: a translational regulator of cell fate. J. Cell Sci. 115, 1355–1359.

Patel, D.J., 1999. Adaptive recognition in RNA complexes with peptides and protein modules. Curr. Opin. Struct. Biol. 9, 74–87.

Potter, C.J., Turenchalk, G.S., Xu, T., 2000. *Drosophila* in cancer research. An expanding role. Trends Genet. 16, 33–39.

Qiu, P., Pan, P., Govind, S., 1998. A role for the *Drosophila* Toll/Cactus pathway in larval hematopoiesis. Development 125, 1909–1920.

Reiter, L.T., Potocki, L., Chien, S., Gribskov, M., Bier, E., 2001. A systematic analysis of human disease-associated gene sequences in *Drosophila melanogaster*. Genome Res. 11, 1114–1125.

Rizki, T.M., Rizki, R.M., 1983. Blood cell surface changes in *Drosophila* mutants with melanotic tumors. Science 220, 73–75.

Russo, J., Brehelin, M., Carton, Y., 2001. Haemocyte changes in resistant and susceptible strains of *D. melanogaster* caused by virulent and avirulent strains of the parasitic wasp *Leptopilina boulardi*. J. Insect Physiol. 47 (2), 167–172.

Shen, H., Kan, J.L., Green, M.R., 2004. Arginine-serine-rich domains bound at splicing enhancers contact the branchpoint to promote prespliceosome assembly. Mol. Cell 13 (3), 367–376.

Sordet, O., Rebe, C., Plenchette, S., Zermati, Y., Hermine, O., Vainchenker, W., Garrido, C., Solary, E., Dubrez-Daloz, L., 2002. Specific involvement of caspases in the differentiation of monocytes into macrophages. Blood 100, 4446–4453.

Spradling, A.C., Stern, D., Beaton, A., Rhem, E.J., Laverty, T., Mozden, N., Misra, S., Rubin, G.M., 1999. The Berkeley Drosophila Genome Project gene disruption project: Single P-element insertions mutating 25% of vital *Drosophila* genes. Genetics 153, 135–177.

Sullivan, W., Ashburner, M., Hawley, R.S., 2000. Drosophila Protocols. Cold Spring Harbor Laboratory Press, New York.

van der Houven van Oordt, W., Diaz-Meco, M.T., Lozano, J., Krainer, A.R., Moscat, J., Caceres, J.F., 2000. The MKK(3/6)-p38-signaling cascade alters the subcellular distribution of hnRNP A1 and modulates alternative splicing regulation. J. Cell Biol. 149 (2), 307–316.

Wang, H.Y., Xu, X., Ding, J.H., Bermingham Jr., J.R., Fu, X.D., 2001. SC35 plays a role in T cell development and alternative splicing of CD45. Mol. Cell 7, 331–342.

Watson, K.L., Konrad, K.D., Woods, D.F., Bryant, P.J., 1992. *Drosophila* homolog of the human S6 ribosomal protein is required for tumor suppression in the hematopoietic system. Proc. Natl. Acad. Sci. U. S. A. 89, 11302–11306.

Wharton, K.A., Cook, J.M., Torres-Schumann, S., de Castro, K., Borod, E., Phillips, D.A., 1999. Genetic analysis of the bone morphogenetic protein-related gene, gbb, identifies multiple requirements during *Drosophila* development. Genetics 152, 629–640.

Wu, J.Y., Maniatis, T., 1993. Specific interactions between proteins implicated in splice site selection and regulated alternative splicing. Cell 75, 1061–1070.